

Optimization of the filter parameters in ^{99m}Tc myocardial perfusion SPECT studies: the formulation of flowchart

Takayuki Shibutani^{1,2} · Masahisa Onoguchi¹ · Tomoki Yamada³ · Hiroki Kamida⁴ · Kohei Kunishita⁵ · Yuuki Hayashi⁶ · Tadashi Nakajima³ · Seigo Kinuya²

Received: 23 February 2015 / Accepted: 28 February 2016 / Published online: 6 April 2016
© Australasian College of Physical Scientists and Engineers in Medicine 2016

Abstract Myocardial perfusion single photon emission computed tomography (SPECT) is typically subject to a variation in image quality due to the use of different acquisition protocols, image reconstruction parameters and image display settings by each institution. One of the principal image reconstruction parameters is the Butterworth filter cut-off frequency, a parameter strongly affecting the quality of myocardial images. The objective of this study was to formulate a flowchart for the determination of the optimal parameters of the Butterworth filter for filtered back projection (FBP), ordered subset expectation maximization (OSEM) and collimator-detector response compensation OSEM (CDR-OSEM) methods using the evaluation system of the myocardial image based on technical grounds phantom. SPECT studies were

acquired for seven simulated defects where the average counts of the normal myocardial components of 45° left anterior oblique projections were approximately 10–120 counts/pixel. These SPECT images were then reconstructed by FBP, OSEM and CDR-OSEM methods. Visual and quantitative assessment of short axis images were performed for the defect and normal parts. Finally, we formulated a flowchart indicating the optimal image processing procedure for SPECT images. Correlation between normal myocardial counts and the optimal cut-off frequency could be represented as a regression expression, which had high or medium coefficient of determination. We formulated the flowchart in order to optimize the image reconstruction parameters based on a comprehensive assessment, which enabled us to perform objectively processing. Furthermore, the usefulness of image reconstruction using the flowchart was demonstrated by a clinical case.

✉ Masahisa Onoguchi
onoguchi@staff.kanazawa-u.ac.jp

Takayuki Shibutani
iwsb03100621@staff.kanazawa-u.ac.jp

- ¹ Department of Quantum Medical Technology, Graduate School of Medical Sciences, Kanazawa University, 5-11-80 Kodatsuno, Kanazawa, Ishikawa 920-0942, Japan
- ² Department of Biotracer Medicine, Graduate School of Medical Science, Kanazawa University, Kanazawa, Japan
- ³ Department of Radiological Technology, Kishiwada City Hospital, 1001 Gakuhara-cho, Kishiwada, Osaka, Japan
- ⁴ Department of Radiological Technology, Higashiosaka City General Hospital, 3-4-5 Nishiiwata, Higashiosaka, Osaka, Japan
- ⁵ Department of Radiological Technology, Osaka Medical Center for Cancer and Cardiovascular Diseases, 1-3-3 Nakamichi, Higashinari-ku, Osaka, Japan
- ⁶ Department of Radiological Technology, Sakai City Medical Center, 1-1-1 Ebaraji, Nishiku, Sakai, Osaka, Japan

Keywords Myocardial perfusion SPECT · Optimization · Standardization · Butterworth filter · Cut-off frequency · Flowchart

Introduction

Myocardial perfusion single photon emission computed tomography (SPECT) is widely used for the diagnosis of ischemic heart disease, myocardial viability, risk stratification, adaptation of revascularization and evaluation of therapy. However, myocardial perfusion SPECT is subject to image quality due to the use of different acquisition protocols, image reconstruction parameters and image display settings among each institution [1]. To standardize these parameters, scientific conferences of various

countries have published guidelines [2–5]. For example, the guidelines of both the Society of Nuclear Medicine and Molecular Imaging (SNMMI) and the European Association of Nuclear Medicine (EANM) have recommended that the necessary average counts to maintain images quality must only be obtained with a minimum of 500,000 counts per each view (a minimum of 400 counts/cm² for normal myocardium) [2, 3]. However, SPECT projections commonly contain uptake other than myocardium (e.g. lung, liver, gallbladder and intestine), which makes it difficult to judge whether these satisfy these guidelines. A guideline of the Japan Society of Nuclear Medicine Technology (JSNMT) has recommended that the average myocardial counts of left anterior oblique (LAO) 45° projection data must have more than 100 counts/pixel [5]. However, these criteria cannot be used for measurement estimation after the examination has taken place. Therefore, actual myocardial counts may contain significant variability due to patient's condition and examination protocols (e.g. injection dose, the intervals from injection until acquisition start, uptake ratio of myocardium and washout rate).

In general, image reconstruction parameters of myocardial perfusion SPECT are subjectively or objectively determined by operators. If image reconstruction parameters are determined subjectively, intra- and inter-operator repeatability decreases. Thus, image reconstruction parameters need to be set objectively to improve operator repeatability. SNMMI and EANM guidelines have recommended that image reconstruction parameters change as a function of injection dose, which should not be varied routinely [2, 3]. However, even if radioactivity dose was identical in all subjects, myocardial counts is inversely proportional to the patient's weight [6].

One of the principal image reconstruction parameters is the Butterworth filter, a parameter strongly affecting the quality of myocardial images. Onishi et al. have reported a procedure to decide optimal Butterworth filter parameters by each collimator from spatial domain and frequency domain assessments using ^{99m}Tc and ²⁰¹Tl agents [7]. Furthermore, they have reported optimal Butterworth filter parameters must change by a difference of radioactivity dose [8, 9]. However, the correlation between the difference of myocardial counts and optimal image reconstruction parameters variability have never been revealed. The objective of this study was to formulate a flowchart to decide optimal Butterworth filter parameters by filtered back projection (FBP), ordered subset expectation maximization (OSEM) and collimator-detector response compensation OSEM (CDR-OSEM) methods [10] using the evaluation system of the myocardial image based on technical grounds (EMIT) phantom [11].

Materials and methods

EMIT phantom design

EMIT phantom was developed to reduce a difference of image quality among institutions [11]. The appearance and myocardial region of the phantom are shown in Fig. 1. The thorax phantom was constructed with an elliptical shape 300 mm in the major axis, 220 mm in the minor axis and a height of 223 mm, which included the lungs containing beads of polystyrene foam and myocardium. Myocardium was constructed from cylinder shapes of 223 mm in height and 80 mm in diameter, and the myocardial thickness and diameter of the left ventricular (LV) chamber were 10 and 40 mm, respectively. The myocardial and LV chamber volumes were approximately 375 and 265 mL, which can fill with liquid such as water and radiopharmaceuticals. Furthermore, the myocardium has normal part and eight defect part with four sizes of defect (5, 10, 15 and 20 mm; thickness and length were constant at 10 and 30 mm) and four thicknesses of defect (10, 7.5, 5 and 2.5 mm; size and length were constant at 20 and 30 mm) simultaneously. The four defects of different sizes were set on same walls with 15 mm interval, and the four defects of different thickness were set on the opposite with contralateral myocardial walls having 15 mm interval. The major characteristic of the phantom was to shift the defect location, so that it can simulate the four patterns: anterior, septal, inferior and lateral walls. Furthermore, the phantom can be used to simulate and acquire eight different defects simultaneously.

Acquisition protocols

SPECT images were obtained using a dual-headed SPECT scanner (Infinia3, GE Healthcare Co., Ltd., Tokyo, Japan). Technetium-99m agent was inserted into the myocardial part of EMIT phantom. SPECT study was acquired using low energy high resolution (LEHR) collimator, 90° apart head configuration, 64 × 64 matrix, 1.6 zoom, 30 projections, circular orbit of 180° rotation and pixel size of 5.52 mm. Normal myocardial counts were determined by average counts obtained from regional of interests (ROI) on the normal myocardial parts of LAO 45° projection data. The average normal myocardial counts were approximately 10, 20, 40, 60, 80, 100 and 120 counts/pixel, which was adjusted by acquisition time. The defect locations were set on four patterns (anterior, lateral, inferior and septal walls of myocardium). Finally, SPECT images were obtained from 28 projection datasets (seven acquisitions of the difference of normal myocardial counts using four different patterns in each acquisition).

Fig. 1 The structure of the evaluation system of myocardial image based on technical grounds (EMIT) phantom. The myocardium and left ventricle (LV) volume are approximately 375 and 265 mL, respectively. **a** The alignment of lungs and myocardium for z axis view. The length of z axis view is 233 mm, the lungs contain polystyrene foam beads. **b** X–Y view alignment. The length of x and y axis views are 300 and 220 mm, respectively. **c** The four sizes of defect (5, 10, 15 and 20 mm; thickness is constant at 10 mm). **d** The four thicknesses of defect (2.5, 5, 7.5 and 10 mm; size is constant at 20 mm)

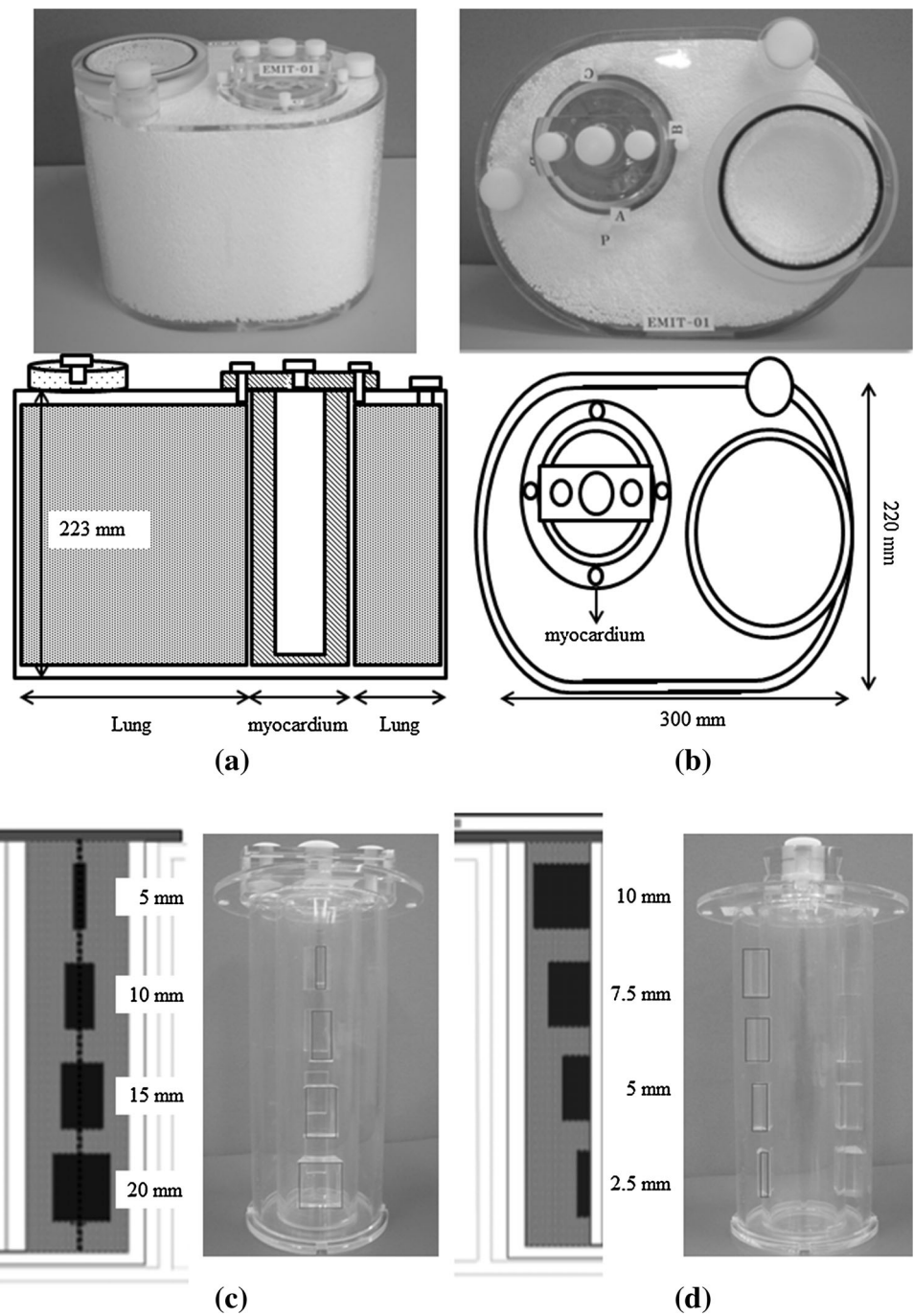


Image reconstruction parameters

The SPECT images were reconstructed by FBP, OSEM and CDR-OSEM methods. The FBP reconstruction was performed with a Ramp filter and the Butterworth filter. Butterworth filter was derived by Eq. 1.

$$B(f) = \sqrt{\frac{1}{1 + (fc/F)^p}} \tag{1}$$

where F indicates the cut-off frequency, and n is the power (constant value: 10). Cut-off frequencies were used for seven patterns of 0.30, 0.35, 0.40, 0.45, 0.50, 0.55 and 0.60 cycles/cm to validate optimal parameters among FBP, OSEM and CDR-OSEM methods. The subset and iteration of OSEM and CDR-OSEM methods used six and five for OSEM method, six and twenty for CDR-OSEM method, respectively. Scatter and attenuation corrections were not employed in all methods.

Image assessments

Short axis images were distinctly examined for defect and normal parts, which were evaluated by visual and quantitative assessments of the defect part and visual assessment of the normal part. The defect sizes using visual and quantitative assessments were 15 mm for FBP and OSEM methods and 10 mm for CDR-OSEM method, and thickness was constant at 10 mm in all methods. The visual

registration was performed between reconstructed SPECT image and template magnetic resonance image (MRI), and a polar map calculated from SPECT image after registration was subsequently generated. Template ROI was created with eight defect parts using MRI, which was set on SPECT polar map after image registration. A profile curve in template ROI was drawn using each defect part on polar map (Fig. 2). The %count of myocardial defects for each size and thickness was calculated in Eq. 2.

$$\%count = \frac{\text{Volume of area under count profile curve of each defect in template ROI}}{\text{Volume of each defect using template ROI decided from MRI}} \times 100 \tag{2}$$

assessment was scored on a scale of 1–5 (5: excellent, 4: good, 3: even, 2: bad, 1: poor) by five observers, and the average score of acceptance criterion defined by a total of more than four points. The quantitative assessment was evaluated using EMIT programs [11]. EMIT programs can work on the windows OS. As the first step, image

The %count defined a defect as less than 2 standard deviations (SD) of normal database of Mid-A, Mid-I, Mid-IL, and Mid-IS. We used a normal database created by Nakajima et al. [12]. The optimal cut-off frequency was determined by comprehensive assessment including visual and quantitative assessments, and created regression

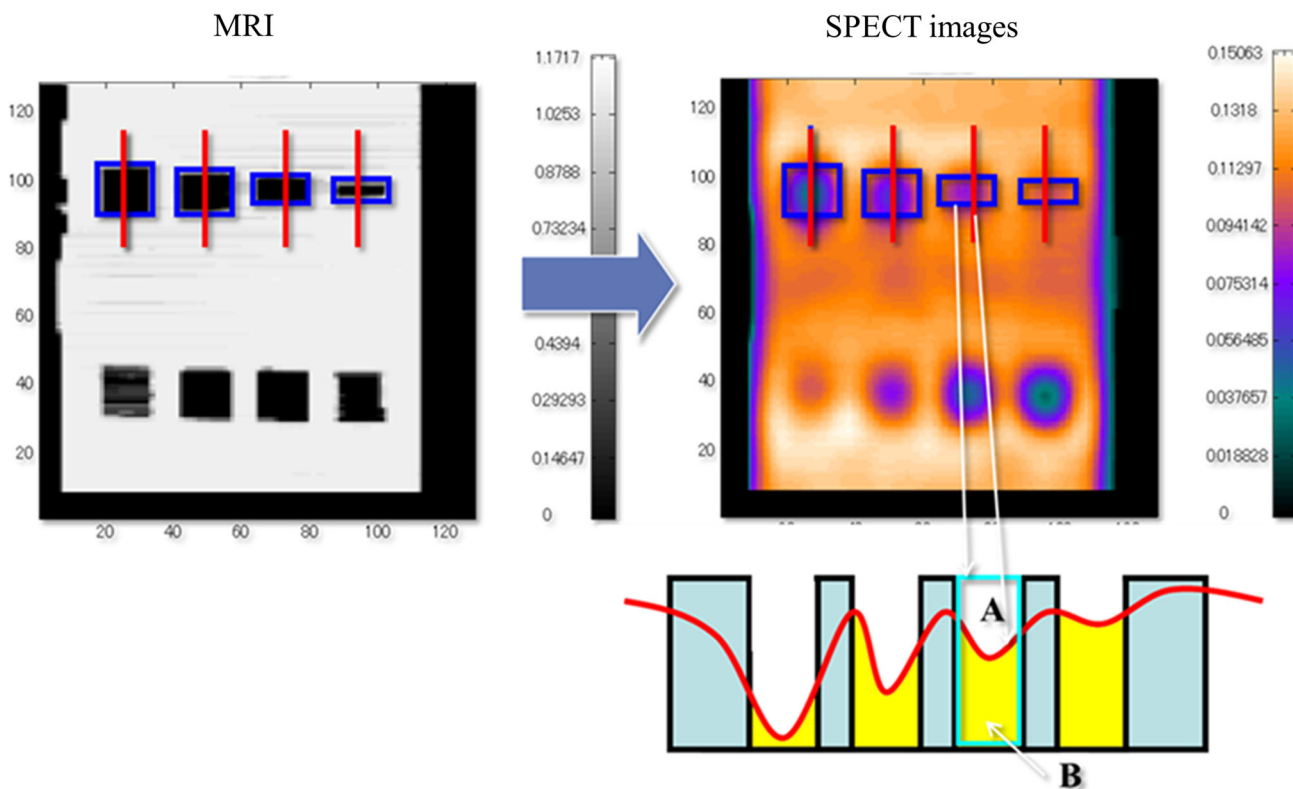


Fig. 2 An algorithm of the evaluation system of the myocardial image based on technical grounds (EMIT) programs. The *left image* indicates the polar map for MRI, and the *right image* is for SPECT. The *blue boxes* indicate the template ROI for each defect size. The profile curve of each defect size is obtained from the four *red lines* in

MRI and SPECT images. The four count profile curves were combined by normalization of max counts. An *aqua box* indicates each defect volume using template ROI determined from MRI, and *yellow areas* indicate the volume of area under the count profile curve of each defect in the template ROI

equations described the correlation between normal myocardial counts and optimal cut-off frequency. Finally, we formulated a flowchart indicating the image reconstruction procedure to optimize SPECT images based on comprehensive assessment. In addition, the utility of the flowchart was validated in retrospectively using clinical studies compared with guidelines. Permission for clinical data used in this study was obtained from the hospital ethics committee.

Results

The visual score of defect assessment for all methods had the optimal cut-off frequency ranges (0.35–0.60 cycles/cm) in all normal myocardial counts (Fig. 3). The %count of FBP and OSEM methods optimized cut-off frequencies of 0.30–0.60 cycles/cm and CDR-OSEM method optimized frequencies of 0.40–0.60 cycles/cm (Fig. 4). Normal assessment had optimal cut-off frequency in normal

Fig. 3 Visual score of defect assessment among three methods (a FBP, b OSEM, c CDR-OSEM). Dotted line indicate acceptance criteria, and error bar describes standard error of the mean

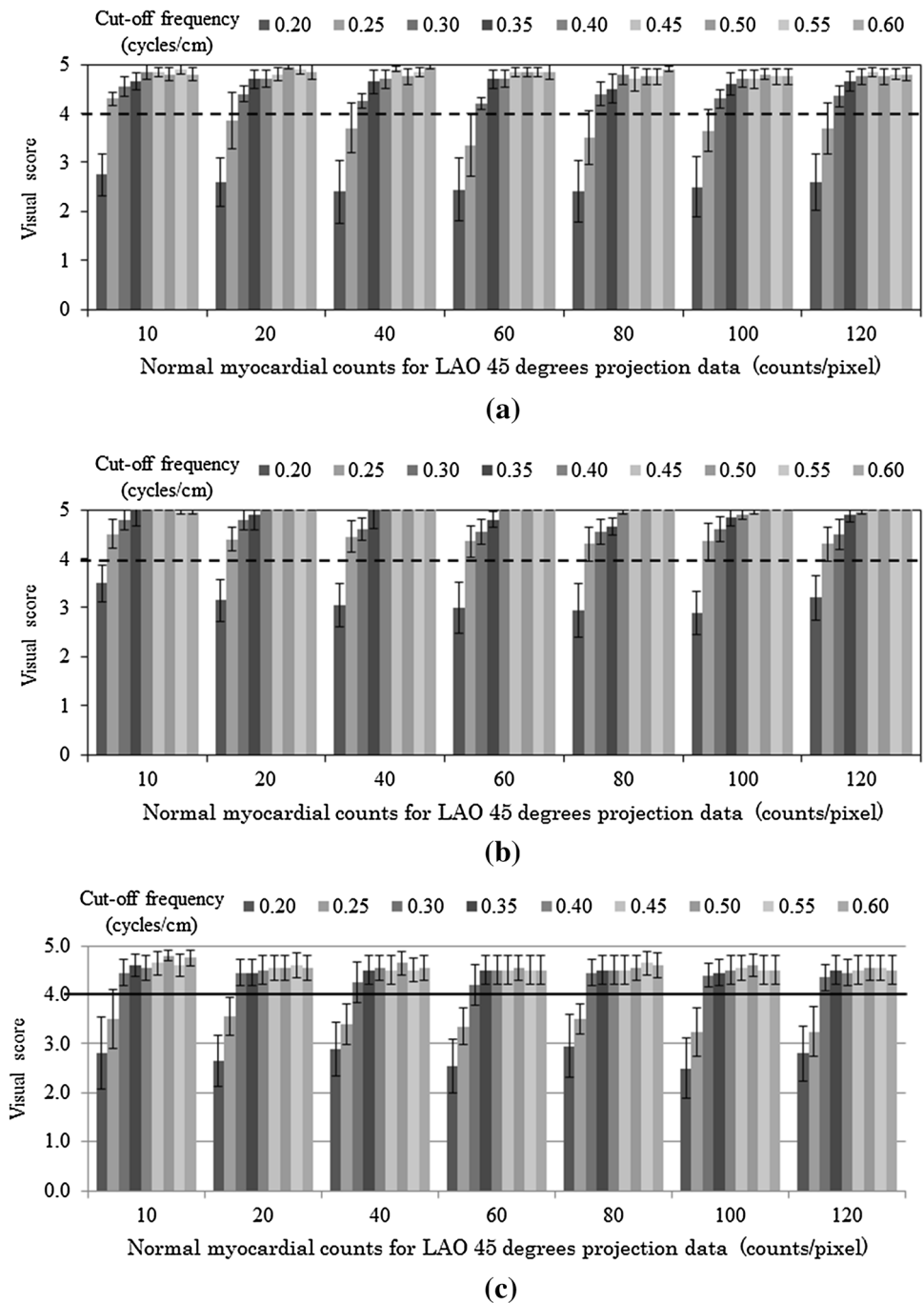
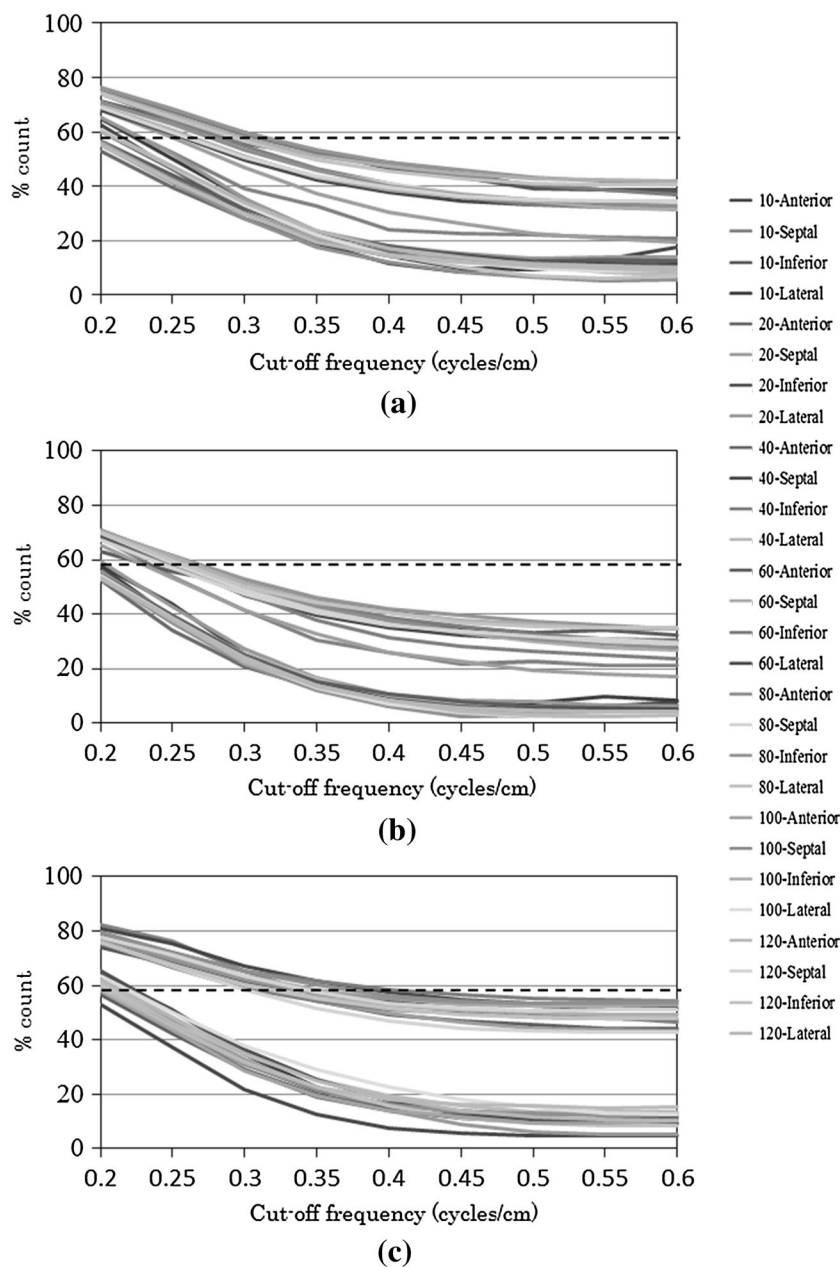


Fig. 4 %count of defect assessment among three methods (a FBP, b OSEM, c CDR-OSEM). Dotted line indicates acceptance criteria

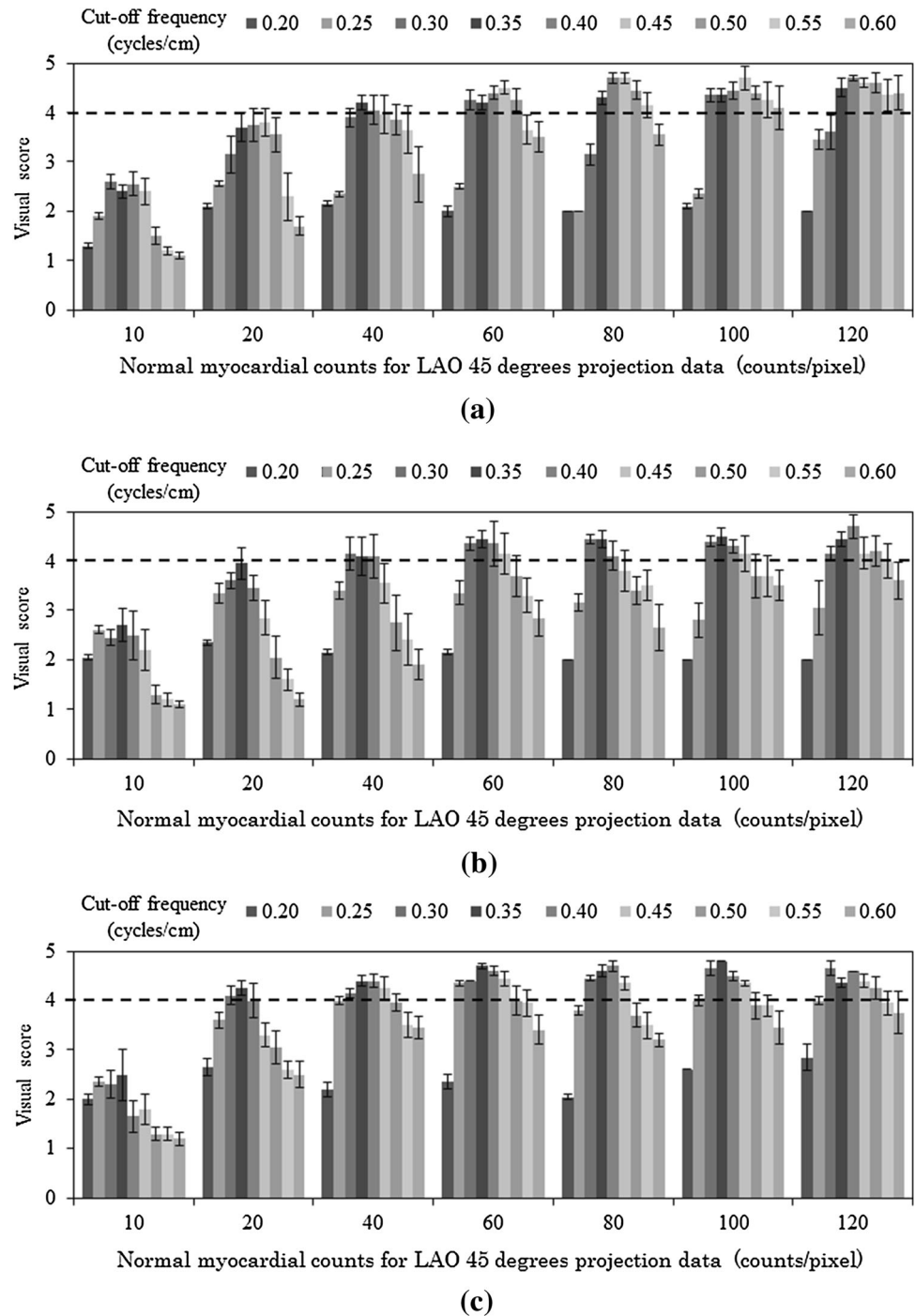


myocardium of 40–120 counts/pixel for FBP and CDR-OSEM methods, and 60–120 counts/pixel for OSEM method. When the normal myocardial count was low, the normal part of the myocardial image was poor, with 10 and 20 counts/pixel for FBP method, 10, 20 and 40 counts/pixel for OSEM method and 10 counts/pixel for CDR-OSEM method (Fig. 5). The optimal cut-off frequency ranges among three methods were determined by a comprehensive assessment including normal and defect parts (FBP: 40, 60, 80, 100 and 120 counts/pixel were 0.35, 0.35–0.45, 0.35–0.50, 0.35–0.50 and 0.35–0.50 cycles/cm, OSEM: 60, 80, 100 and 120 counts/pixel were 0.30–0.35, 0.30–0.40 and 0.35–0.40 cycles/cm, CDR-

OSEM: 40, 60, 80, 100 and 120 counts/pixel were 0.35–0.40, 0.40–0.45, 0.35–0.45, 0.40–0.45 and 0.35–0.45 cycles/cm). However, the 10 and 20 counts/pixel for the FBP and CDR-OSEM methods and the 10, 20 and 40 counts/pixel of the OSEM method had no optimal cut-off frequency ranges.

The correlation between optimal cut-off frequencies and normal myocardial counts are shown in Fig. 6. Correlation between normal myocardial counts and optimal cut-off frequency could be represented as regression equations in all methods, which had high or medium coefficient of determination as follows: FBP: $y = -0.0000446x^2 + 0.00889x + 0.07$, $R^2 = 0.98$, OSEM: $y = 0.001x + 0.285$,

Fig. 5 Visual score of normal assessment among three methods (a FBP, b OSEM, c CDR-OSEM). Dotted line indicates acceptance criteria, and error bar describes standard error of the mean



$R^2 = 0.80$, CDR-OSEM: $y = -0.000018x^2 + 0.0031x + 0.55$, $R^2 = 0.55$, where x and y indicate optimal cut-off frequency and normal myocardial counts, respectively. We formulated a flowchart to optimize image reconstruction parameters based on comprehensive assessment to improve inter- and intra-operator reproducibility (Fig. 7). Myocardial short axis images were created using optimal cut-off frequency guided from the flowchart procedure, so that those images correctly described defect and normal parts (Fig. 8).

Case report

An 80-year-old woman was referred to our department for exercise myocardial perfusion SPECT because of suspected angina pectoris. She had been treated for diabetes mellitus and hypertension. The radiopharmaceutical agent of ^{99m}Tc -tetrofosmin 296 MBq was injected at the half time during the six minutes adenosine infusion, and myocardial perfusion SPECT acquisition was undertaken

Fig. 6 Correlation between cut-off frequency and normal myocardial counts among three methods. All methods were represented as regression equations, which had high or medium coefficient of determination

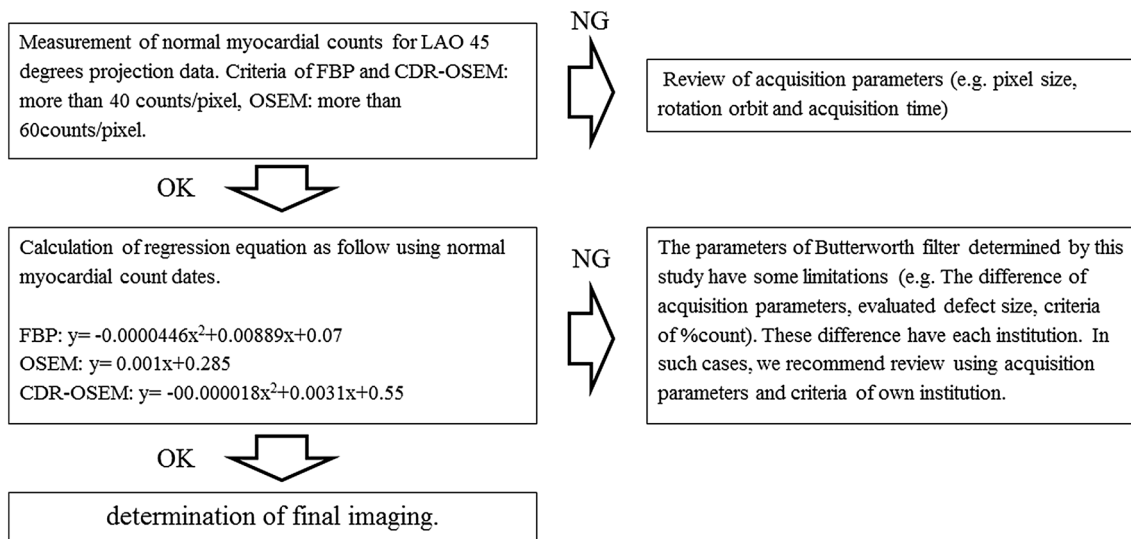
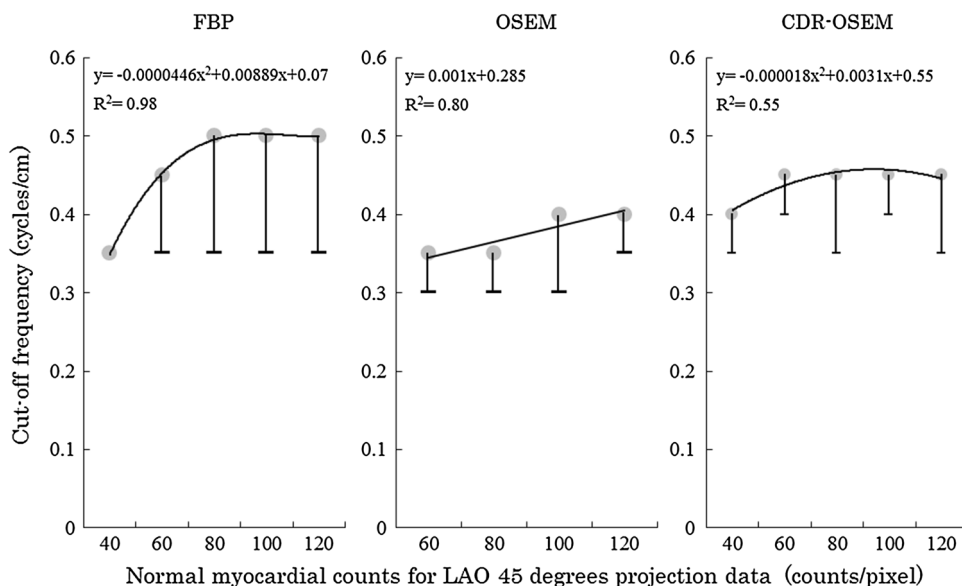


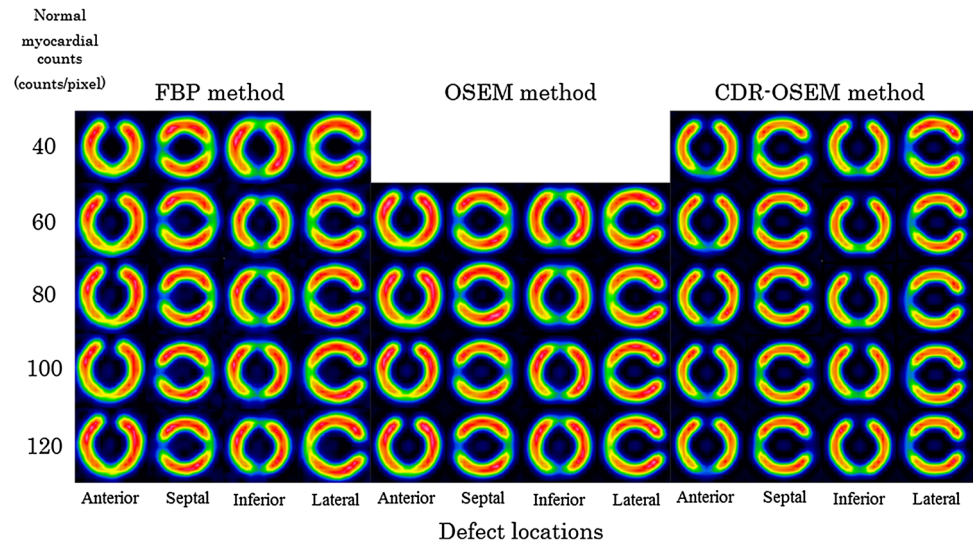
Fig. 7 A flowchart to indicate image reconstruction procedure to optimize the cut-off frequency based on comprehensive assessment. The first section confirms normal myocardial counts. If normal myocardial counts have less than 40 counts/pixel for FBP and CDR-OSEM methods or 60 counts/pixel for OSEM method, we

recommend re-examination by changing the acquisition parameters. The next section recommends processing the projection data using regression equations, and thereby determining the final images. If it has a problem with image quality, an explanation of the regression equations is warranted

with the patient in the supine position after a 30 min injection. The imaging was performed with a dual-head gamma-camera equipped with a LEHR collimator, and energy windows were $140 \text{ keV} \pm 10 \%$. The projection data was acquired in 30 steps around a 180° arc for 40 s per projection starting with the right anterior oblique view and ending with the left posterior oblique view. The total acquisition time was approximately 12 min. The acquisition was in step-and-shoot mode with a zoom factor of 1.6, and the images were recorded in a 64×64 matrix (pixel

size: 5.52 mm). In addition, a coronary angiography (CAG) was performed after 8 days, and results of CAG showed significant stenosis on the proximal and middle of the right coronary artery, in addition to the distal and first diagonal branch of the left coronary artery. Myocardial images were processed by means of the guideline and the flowchart as shown in Fig. 9 (a: Guideline, b: FBP, c: OSEM, d: CDR-OSEM). Normal myocardial counts in this case had the 79 counts/pixel. In FBP, OSEM and CDR-OSEM methods, myocardial images had a mild hypo-

Fig. 8 Myocardial images processed using the optimal cut-off frequency using three methods. These images indicate myocardial image slice used for normal and defect assessments regarding three methods. All of the images have described correctly the defect and normal locations



perfusion area in the mid and apical anterior walls, basal and mid inferior walls. However, the myocardial images based on EANM guidelines showed no hypo-perfusion areas.

Discussion

Myocardial perfusion SPECT is widely used for diagnosis of ischemic and viability, risk stratification, adaptation of revascularization and therapy evaluation [13]. In particular, it plays an important role in diagnosis of angina pectoris and myocardial infarction, which is used to judge whether medical therapy or revascularization is required [14]. However, myocardial perfusion SPECT study produces different images depending on the different acquisition protocols, image reconstruction parameters and image display settings used by each institution, which has been reported in a study [1]. Therefore, it is possible to generate the artifact, so that the myocardial image generates a false-positive or false-negative. Butterworth filter parameter setting is possibly one of the causes of the artifacts, which has to set for each patient. However, optimal parameters for each patient have not been investigated in detail in previous studies. Therefore, we have attempted to determine optimal image reconstruction parameters using normal myocardial counts in this study.

Normal myocardial count ranges are determined in reference to clinical studies. In addition, to validate optimal Butterworth filter parameters, cut-off frequency ranges were set to 0.20–0.60 cycles/cm corresponding to 20–70 % of the Nyquist frequency, which was determined by the ranges in reference to past studies [7–9]. The subset and iteration of reconstruction parameters for OSEM and CDR-

OSEM methods were determined from past studies [15–18]. Furthermore, Maru and Yanagisawa have reported that it was not necessary to change subset and iteration by the difference of acquisition counts [19]. Thus, we did not change subset and iteration in this study. The estimated defect size among three methods were determined by full width at half maximum (FWHM) from a phantom study based on National Electrical Manufacturers Association (NEMA) [20]. Estimated defect sizes in this study were determined as 15 mm for FBP and OSEM methods, 10 mm for CDR-OSEM method corresponding to the smallest size in defect size more than the FWHM which is 11.8, 11.4 and 5.3 mm for FBP, OSEM and CDR-OSEM methods, respectively. The %count defined a defect as less than 2 SD of the normal database in our study. The %count theoretical value is normally 0 % in all of myocardial walls in order to simulate a complete defect. However, these criteria have taken into account the influence of both partial volume effect and limitation of spatial resolution. However, to approximate the %count theoretical value, the optimal cut-off frequency by normal myocardial counts determined the highest of cut-off frequency ranges as indicated by comprehensive assessment. Normal myocardial counts needed for optimal imaging was a minimum of 40 counts/pixel for FBP and CDR-OSEM method or 60 counts/pixel for OSEM method. The OSEM algorithm has a characteristic of enhancing statistical noise when normal myocardial counts are less, so that it was required to obtain higher normal myocardial counts as compared to other methods. However, the CDR-OSEM method could provide optimal image until lower counts in spite of OSEM algorithm. The CDR-OSEM method has reconstructed using maximum a posteriori-expectation maximization (MAP-EM) algorithm incorporates Bayes' theorem, which reportedly decreases

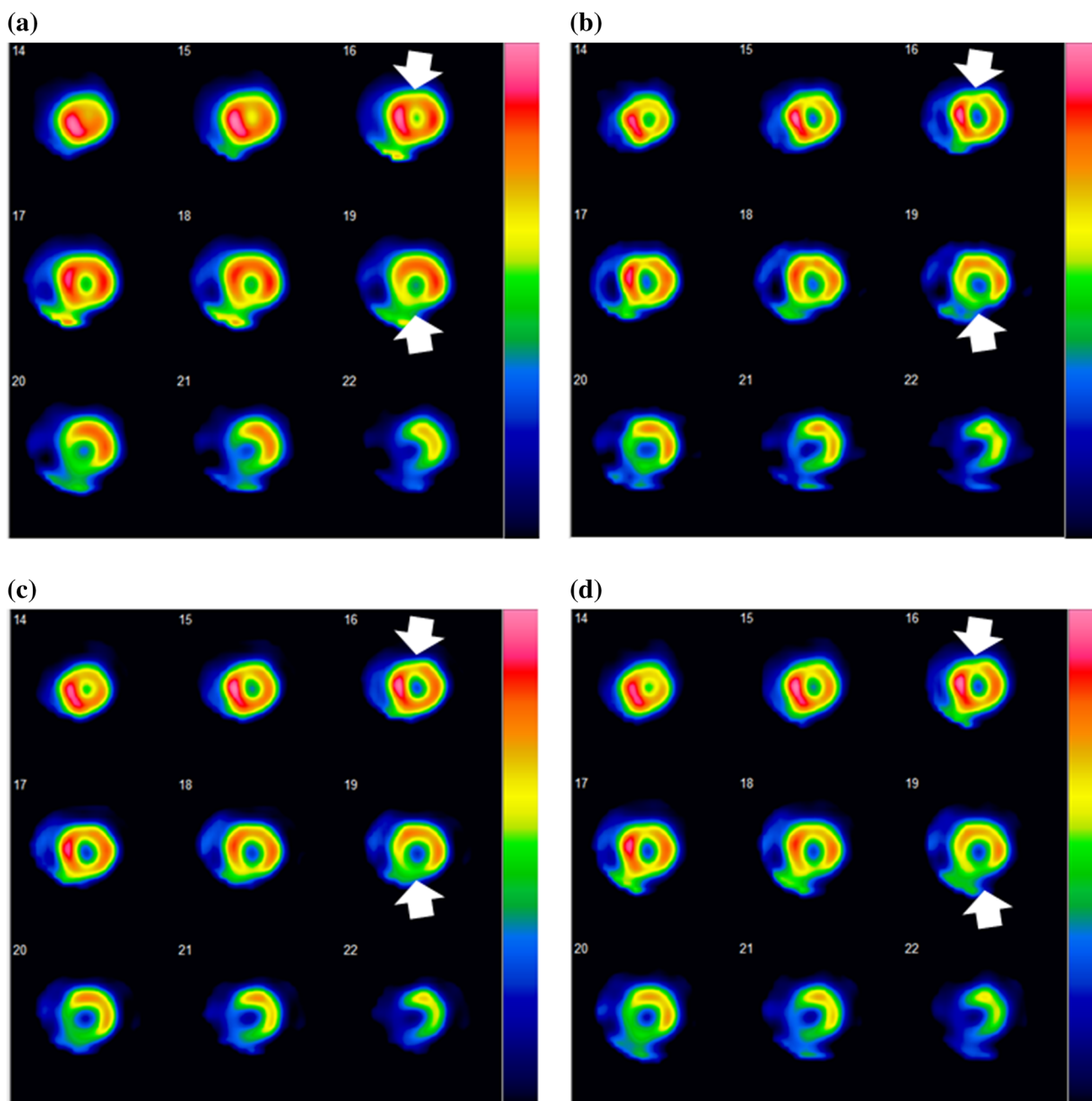


Fig. 9 Short axis images of myocardial perfusion SPECT (**a** guideline, **b** FBP, **c** OSEM, **d** CDR-OSEM). Normal myocardial counts in this case had 79 counts/pixel. Myocardial images processed using the

flowchart had a mild hypo-perfusion area in the mid and apical anterior walls, basal and mid inferior walls. However, myocardial images using the EANM guidelines showed no hypo-perfusion areas

the statistical noise [21]. Therefore, the CDR-OSEM method had optimal image until lower counts, a higher cut-off frequency than OSEM method. The correlation between normal myocardial counts and optimal cut-off frequency was expressed as regression equations by three methods. Furthermore, we formulated a flowchart to produce optimal image quality using regression equations. Consequently, the flowchart allowed us to objectively process against different normal myocardial counts.

In the clinical case, we performed image reconstruction using EANM guidelines and the flowchart. Myocardial images reconstructed using EANM guidelines tended to reduce the detection of anterior and inferior walls, whereas myocardial images reconstructed using the flowchart incorporating the three methods detected mild hypo-perfusion of the anterior and inferior walls. As a result of this case, we could demonstrate the usefulness of the image reconstruction using the flowchart.

Our study has some limitations. Firstly, the EMIT phantom does not simulate scatter and attenuation, however human bodies are susceptible to the effects of scatter and attenuation. Should a phantom simulate these effects, the flowchart may need to be changed. Furthermore, different acquisition parameters were not validated in this study, however, Onishi et al. have reported that on varied optimal image reconstruction parameters by different acquisition parameters [7–9]. These limitations will be validated in the next study.

Conclusion

We formulated a flowchart to optimize cut-off frequency among three methods using the EMIT phantom, and were able to determine the optimal cut-off frequency for normal myocardial counts. Furthermore, the usefulness of image reconstruction using the flowchart was demonstrated by a clinical case. Finally, it has been possible to objectively process image reconstruction using the flowchart.

Conflict of interest The authors declare that they have no conflict of interest.

References

- Heikkinen J, Ahonen A, Kuikka JT, Rautio P (1999) Quality of myocardial perfusion single-photon emission tomography imaging: multicentre evaluation with a cardiac phantom. *Eur J Nucl Med* 26:1289–1297
- William Strauss H, Douglas Miller D, Wittry MD, Cerqueira MD, Garcia EV, Iskandrian AS, Schelbert HR, Wackers FJ, Balon HR, Lang O et al (2008) Procedure guideline for myocardial perfusion imaging 3.3. *J Nucl Med Technol* 36:155–161
- Hesse B, Tägil K, Cuocolo A, Anagnostopoulos C, Bardiès M, Bax J, Bengel F, Busemann Sokole E, Davies G, Dondi M et al (2005) EANM/ESC procedural guidelines for myocardial perfusion imaging in nuclear cardiology. *Eur J Nucl Med Mol Imaging* 32:855–897
- Holly TA, Abbott BG, Al-Mallah M, Calnon DA, Cohen MC, DiFilippo FP, Ficaro EP, Freeman MR, Leonard SM, Nichols KJ et al (2010) Single photon-emission computed tomography. *J Nucl Cardiol* 17:941–973
- Working Group for Investigation and Research on Nuclear Medicine Image Quantification and Standardization, Japanese Society of Nuclear Medicine Technology (2008) Point of acquisition, processing, display and output for standardized images with clinical usefulness. *Jpn J Nucl Med Technol* 28:13–66
- O'Connor MK, Bothun E, Gibbons RJ (1998) Influence of patient height and weight and type of stress on myocardial count density during SPECT imaging with thallium-201 and technetium 99m-sestamibi. *J Nucl Cardiol* 5:304–312
- Onishi H, Matsutake Y, Matsutomo N, Amijima H (2010) Validation of optimal cut-off frequency using a Butterworth filter in single photon emission computed tomography reconstruction for the target organ: spatial domain and frequency domain. *Humanity Sci* 10:27–36
- Onishi H, Ushio T, Matsuo S, Takahashi M, Noma K, Masuda K (1996) Optimized Butterworth filters for ^{99m}Tc myocardial perfusion SPECT images: an evaluation. *Jpn J Radiol Technol* 52:346–350
- Onishi H, Ota T, Takada M, Kida T, Noma K, Matsuo S, Masuda K, Yamamoto I, Morita R (1997) Two optimal prefilter cutoff frequencies needed for SPECT images of myocardial perfusion in a one-day protocol. *J Nucl Med Technol* 25:256–260
- GE Healthcare (2011) Evolution for cardiac white paper. http://www3.gehealthcare.com/en/products/categories/nuclear_medicine/xeleris_workstations_and_applications/evolution_for_cardiac. Reference: 20 Feb 2015
- Onoguchi M, Katafuchi T, Yoshioka K (2011) Development of a myocardial phantom and analysis system toward standardization of myocardial SPECT image. *J Nucl Med* 52(Suppl 1):2358
- Nakajima K, Kumita S, Ishida Y, Momose M, Hashimoto J, Morita K, Taki J, Yamashina S, Maruno H, Ogawa M et al (2007) Creation and characterization of Japanese standards of myocardial perfusion SPECT: database from the Japanese Society of Nuclear Medicine Working Group. *Ann Nucl Med* 21:505–511
- JCS Joint Working Group (2012) Guidelines for clinical use of cardiac nuclear medicine—digest version. *Circ J* 76:761–767
- Yamashina A, Ueshima K, Kimura K, Kuribayashi Y, Sakuma H, Tamaki N, Yoshida K (2009) Guidelines for noninvasive diagnosis of coronary artery lesions. *Circ J* 73(Suppl III):1019–1089
- Seret A (2006) The number of subsets required for OSEM reconstruction in nuclear cardiology. *Eur J Nucl Med Mol Imaging* 33:231
- Ali I, Ruddy TD, Almgrahi A, Anstett FG, Glenn Wells R (2009) Half-time SPECT myocardial perfusion imaging with attenuation correction. *J Nucl Med* 50:554–562
- Hughes T, Celler A (2012) A multivendor phantom study comparing the image quality produced from three state-of-the-art SPECT–CT systems. *Nucl Med Commun* 33:663–670
- Yanagisawa M, Maru S (2001) Study of the OSEM algorithm in myocardial gated SPECT optimization of reconstruction parameters. *Jpn J Radiol Technol* 57:1240–1247
- Maru S, Yanagisawa M (2001) Basic evaluation of OSEM algorithm by assessing iteration times and number of subsets in a hot spot phantom study. *Jpn J Radiol Technol* 57:1233–1239
- National Electrical Manufacturers Association (NEMA) (2012) Performance measurement of gamma cameras. *NEMA NU* 1:42–44
- Green PJ (1990) Bayesian reconstructions from emission tomography data using a modified EM algorithm. *IEEE Trans Med Imaging* 9:84–93